Microstructure and magnetic properties of magnetic fluids consisting of shifted dipole particles under the influence of an external magnetic field

Rudolf Weeber, Marco Klinkigt, Sofia Kantorovich, and Christian Holm

Citation: The Journal of Chemical Physics **139**, 214901 (2013); doi: 10.1063/1.4832239
View online: http://dx.doi.org/10.1063/1.4832239
View Table of Contents: http://scitation.aip.org/content/aip/journal/jcp/139/21?ver=pdfcov
Published by the AIP Publishing

Microstructure and magnetic properties of magnetic fluids consisting of shifted dipole particles under the influence of an external magnetic field

Rudolf Weeber,[1,a)] Marco Klinkigt,[1,b)] Sofia Kantorovich,[2,3,c)] and Christian Holm[1,d)]
[1]*Institut für Computerphysik, Universität Stuttgart, Allmandring 3, 70569 Stuttgart, Germany*
[2]*Ural Federal University, Lenin av. 51, 620083 Ekaterinburg, Russia*
[3]*Universität Wien, Sensengasse 8, 1090 Wien, Austria*

(Received 5 August 2013; accepted 6 November 2013; published online 2 December 2013)

We investigate the structure of a recently proposed magnetic fluid consisting of shifted dipolar (SD) particles in an externally applied magnetic field via computer simulations. For standard dipolar fluids the applied magnetic field usually enhances the dipole-dipole correlations and facilitates chain formation whereas in the present system the effect of an external field can result in a break-up of clusters. We thoroughly investigate the origin of this phenomenon through analyzing first the ground states of the SD-particle systems as a function of an applied field. In a second step we quantify the microstructure of these systems as functions of the shift parameter, the effective interaction parameter, and the applied magnetic field strength. We conclude the paper by showing that with the proper choice of parameters, it is possible to create a system of SD-particles with highly interacting magnetic particles, whose initial susceptibility is below the Langevin susceptibility, and which remains spatially isotropic even in a very strong external magnetic field. © *2013 AIP Publishing LLC*. [http://dx.doi.org/10.1063/1.4832239]

I. INTRODUCTION

In order to create a liquid, which properties might be effectively controlled by an externally applied magnetic field, one needs to suspend magnetizable or magnetic particles in a non-magnetic carrier. Ferrofluids, also called magnetic fluids, are one class of such materials.[1] The particles in ferrofluids consist of ferro- or antiferromagnetic material in a size range from 5 to 50 nm. This is smaller than the size of a single ferromagnetic domain, thus each particle has a permanent magnetic dipole moment. In the absence of an external magnetic field, the particles are randomly oriented due to Brownian motion. Consequently, the ferrofluid as a whole has no net magnetization. When, on the other hand, a field is applied, the magnetic moments of the particles tend to coalign with an applied field and the fluid becomes magnetized. The presence of an applied field leads to a strong change in the ferrofluid's static and dynamic properties.

The investigation of ferrofluid magnetic properties started more than 50 years ago, and comprises an extreme variety of experimental,[2–10] theoretic,[11–23] and computer simulations[24–35] studies. The findings of these studies can be summarised as follows: (1) there are various mechanism with which the magnetic particle might respond to an external magnetic field, namely, Neél (the dipole rotate within the particle to coalign with an applied field, inherent to smaller particles, grows with particle size and depends on the particle material) and Brownian (the particle rotates as a whole to adjust its dipole moment to the direction of the field, inherent to bigger particles, grows with the volume of the particle and carrier viscosity); (2) the characteristic magnetic relaxation time of the ferrofluid depends on the magnetic particle size distribution; (3) there is no ferrofluid which exhibits an initial susceptibility lower than the one of the Langevin law;[36] (4) the stronger the inter-particle interaction is, the higher is the magnetic susceptibility of the system; (5) an external magnetic field strongly enhances the chain formation, and for higher fields even magnetic fluids with moderately interacting particles become strongly aggregated. All these features influence viscous,[7,37–41] optical,[2–4,42–44] diffusion,[6,45] scattering,[45–52] thermodynamic,[22] and acoustic[53] properties of ferrofluids. These systems are widely used in medicine, e.g., actuators[55–57] or sensors for the monitoring of anti-body reactions.[58]

In the vast majority of ferrofluids, the nano-particles are spherical and the field they create can be approximated by that of a point dipole at the sphere's center. In order to achieve a strong coupling between the dipole moment of the particle and an external field, one needs to make particles more magnetic. Such systems at low density will be strongly aggregated. This is not necessarily an advantage for magnetophoretic-based applications such as drug delivery.[54] Thus, one might want to create a system which can be strongly magnetized on the one hand, and be spatially isotropic on the other.

Two possibilities are available to further tailor the characteristics of ferrofluids. First, it is possible to use a more complex carrier, as for instance a polymer gel.[59–62] Second, it is possible to change the fluids properties by modifying the nano-particles. We follow the second route here. In recent years, many types of unusual magnetic systems have been studied. Among them are magnetic rods

a)weeber@icp.uni-stuttgart.de
b)marco.klinkigt@me.com
c)sofia.kantorovich@univie.ac.at
d)holm@icp.uni-stuttgart.de

and ellipsoids,[63,64] magnetic core-shell particles,[65] extended dipoles in the form of two overlapping, oppositely charged spheres,[66] linear molecules with shifted dipoles,[67] particles with magnetic caps,[68] particles interacting by higher moments then dipoles,[69] shifted-dipole particles moving in precessing magnetic fields,[70] and particles with embedded magnetic cubes.[71]

Recently, we proposed an alternative way for creating a system with "unusual" properties.[72–74] These works were inspired by a study of particles with magnetic caps[68] but also show a strong similarity to particles with embedded magnetic cubes.[71] In our model, the particles are spherical but the dipole moment is not located at their centres. Rather, it is shifted radially towards the particle surface, therefore we called them shifted dipolar particles (SD-particles). This leads to a strongly different microstructure and, as shown in this contribution, also to highly different responses to an externally applied magnetic field. In previous studies, the ground states for SD-particles and the microstructure of suspensions in the field-free case have been studied and a comparison to the particles with magnetic caps has been made. In a recent contribution a mean-field Hamiltonian with interesting properties has been constructed for this system.[75]

The paper is organized as follows: in Sec. II, we introduce the SD-particle system in detail, in Sec. III we discuss the ground states of two SD-particles in an external magnetic field. Section IV is concerned with the microstructure and magnetization properties of a suspension of SD-particles at finite temperature. Finally, we conclude with a summary.

II. THE SD-PARTICLE SYSTEM

In computer simulations and analytical studies, magnetic nano-particles are typically treated as soft or hard spheres with a point dipole located at their centre. Hence, magnetically they interact by the dipole-dipole interaction,

$$U_{dd}(\mathbf{m_i}, \mathbf{m_j}, \mathbf{r_{ij}}) = -\frac{\mu_0}{4\pi}\left[3\frac{(\mathbf{m_i}\cdot\mathbf{r_{ij}})(\mathbf{m_j}\cdot\mathbf{r_{ij}})}{r^5} - \frac{(\mathbf{m_i}\cdot\mathbf{m_j})}{r^3}\right]. \tag{1}$$

Here, $\mathbf{m_{i,j}}$ denote the magnetic moments of particles i, j, $\mathbf{r_{ij}}$ stands for the distance between the particles centres, and μ_0 is the vacuum permittivity. The strength of the dipole-dipole interaction is typically measured by the quantity

$$\lambda = \frac{\mu_0 m^2}{4\pi d^3 k_B T}, \tag{2}$$

where d denotes the particles' diameter and k_BT is the thermal energy. Hence, this quantity compares the modulus of the minimum of the dipole-dipole interaction between two particles at close contact to the thermal energy. If λ is on the order of one or smaller the system remains spatially isotropic, i.e., the dipole-dipole interaction is too weak to lead to any particle aggregation. The latter takes place for higher values of λ and the aggregates tend to have linear chain-like shape due to the anisotropy of the magnetic dipole-dipole interaction in Eq. (1) which favors the head-to-tail orientation of particles. The formation of chains is strongly facilitated by the externally applied magnetic field $\mathbf{H}$, as each dipole tries to coalign with it due to the field-dipole interaction (Zeeman energy):

$$U_{iH} = -\mu_0(\mathbf{m_i}\cdot\mathbf{H}). \tag{3}$$

The steric interaction between the particles is usually purely repulsive as the van der Waals interactions are screened by the polymer coating on their (magnetic particle) surface. In this paper, we use a hard sphere interaction for the Monte Carlo investigations of the ground states discussed in Sec. III:

$$U_{\mathrm{HS}}(r) = \begin{cases} \infty, & r \le d \\ 0, & r > d\,, \end{cases} \tag{4}$$

and a purely repulsive Lennard-Jones potential, the so-called WCA potential, for the molecular dynamics simulations in the remaining sections:[76]

$$U_{WCA}(r) = \begin{cases} 4\varepsilon\left[\left(\frac{\sigma}{r}\right)^{12} - \left(\frac{\sigma}{r}\right)^{6} + \frac{1}{4}\right], & r \le d \\ 0, & r > d\,. \end{cases} \tag{5}$$

Here, r is the distance between the center of the particles and $d = 2$ is the particles' diameter. The parameter ϵ was chosen to be 1000. With this choice of parameters, the result is very close to the hard sphere case.

Shifted-dipole particles are different from the usual model of a magnetic nano-particle in that the dipole moment is not located at the particles' centre but rather shifted radially outwards towards their surface. The shift is measured by the parameter s, which denotes the dipole's distance from the particle's centre normalized by the particle radius. Hence, $s = 0$ refers to a particle with central dipole and $s = 1$ refers to the dipole being located at the particle's surface.

Due to the additional anisotropy caused by the non-central dipole, the distance between the dipole moments of adjacent particles now depends on the particles' orientation. As the distance enters in the dipole-dipole interaction in Eq. (1) in the third power, this strongly changes the interaction potential, leading to very different ground states and also different microstructures at finite temperature.

The dipoles can get much closer to each other at high shifts s. Thus, the energy scales for a fixed magnetic moment can be very different and depend on the value of the shift parameter s. To keep simulations with different shifts and external fields comparable in term of the ground state energies, we adjust the employed magnetic moment according to the following scalings.

1. Let $U_{gs}(s)$ be the ground state energy (the lowest possible energy at 0 K) for two SD-particles with a shift of s.
2. The dipole moments are scaled such that the ground state energy for two SD-particles is independent of the shift, i.e.,

$$m(s) = \frac{m(0)}{\sqrt{U_{gs}(s)/U_{gs}(0)}}. \tag{6}$$

At a temperature larger than zero, we define the effective interaction parameter

$$\lambda^* = \frac{\lambda U_{gs}(s)}{U_{gs}(0)}. \quad (7)$$

The parameter λ^* compares the lowest energy for two SD-particles at close contact for a given shift to the thermal energy.

3. The Langevin parameter is defined as the field interaction with the actual magnetic moment $m(s)$ with respect to the thermal energy, and is therefore defined as

$$\alpha = \frac{\mu_0 m(s) H}{k_b T}. \quad (8)$$

4. For the ground states, the dimensionless magnetic field is written in terms of the scaled dipole moment for the given shift relative to the ground state energy for two particles for the given shift,

$$H^* = \frac{\mu_0 m(s) H}{U_{gs}(s)}. \quad (9)$$

III. GROUND STATES

The ground states of small clusters of shifted-dipole particles have been studied using Monte Carlo simulated annealing in Ref. 72–74. Simulated annealing is a heuristic technique to find configurations with minimal energy: a Monte Carlo simulation is performed using the Metropolis algorithm,[77] but the temperature is decreased over time. In this way, a large part of the phase space is sampled at the beginning of the simulation and the system converges to an energy minimum at its end. As the method is not guaranteed to yield the global minimum, many simulations are started for each set of parameters, and the one with the lowest final energy is selected. More technical details can be found in Ref. 72.

For two particles with central dipoles (i.e., $s = 0$), the ground state is the so-called "head-to-tail" configuration, in which the dipole moments of the particles are aligned parallel to each other and to the vector connecting the particles' centres. The "antiparallel side-by-side" configuration, in which the dipole moments are aligned anti-parallel and are orthogonal to the vector connecting the particles' centres is a local minimum.

The outwards shift of the dipole moment ($s > 0$) has a strong influence on the ground states. It was shown analytically and in simulations that three regimes can be observed.[72] For a shift of up to $s = 0.408$, the "head-to-tail" configuration still is the ground state for SD-particles. For $0.408 < s < 0.597$, the two dipole moments rotate inward in a non-symmetric fashion. At the end of this regime, the dipole moments are aligned anti-parallel. For even higher shifts, they rotated inward symmetrically, getting closer and closer to each other.

Let us now summarize the results for larger clusters. For particles with a central dipole, the ground states are chains for up to three particles and rings for four and more particles.[78]

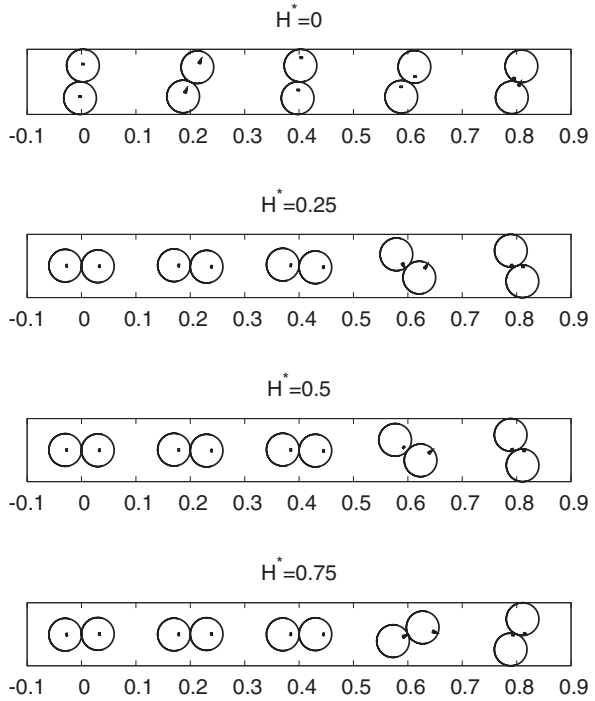

FIG. 1. Ground states of two SD-particles for fields of $H^* = 0$ to 0.75. Only at high shifts the dipoles assume the anti-parallel alignment and the clusters rotate such that the axis connecting the particles' centers is oriented perpendicular to the external field. This transition occurs at higher shifts, when the external field is stronger. (Compare the first and last row).

For SD-particles with a small shift, a ring remains the ground state. At intermediate and high shifts, the particles arrange into hexagonally close-packed structures. While the dipoles align mostly into triangles for intermediate shifts, they form anti-parallel pairs at high shifts. Pictures can be found in Refs. 72 and 74.

Next, we investigate the ground states of two SD-particles in a field. This will help to understand the results for magnetization and cluster structure at room temperature presented in Secs. IV A–IV C, since the ground states structures are often still present as intermediate states in suspensions at finite temperature. Snapshots of the two particle ground states are shown in Fig. 1. When a field is applied, the head-to-tail configuration is the ground state for low shifts. When the shift is increased, the clusters rotate such that the axis connecting the particles' centers is aligned more and more perpendicular to the external field. At the same time, the dipole moments rotate towards each other but keep a component parallel to the external field in order to minimize the Zeeman energy. At very high shifts, the dipoles assume an anti-parallel alignment. At this point, the energy of the ground state no longer depends on the orientation of the vector connecting the particles' centers (r_{12}). Hence, the respective dot product jumps in Fig. 2. The dipoles assume an anti-parallel alignment, because at very high shifts, the advantage of the anti-parallel dipole orientation due to the dipolar interaction energy exceeds the energetic disadvantage of an unfavorable alignment with respect to the external field. To achieve a more detailed understanding of the ground state configurations, the dot product between the two magnetic moments versus the shift is shown

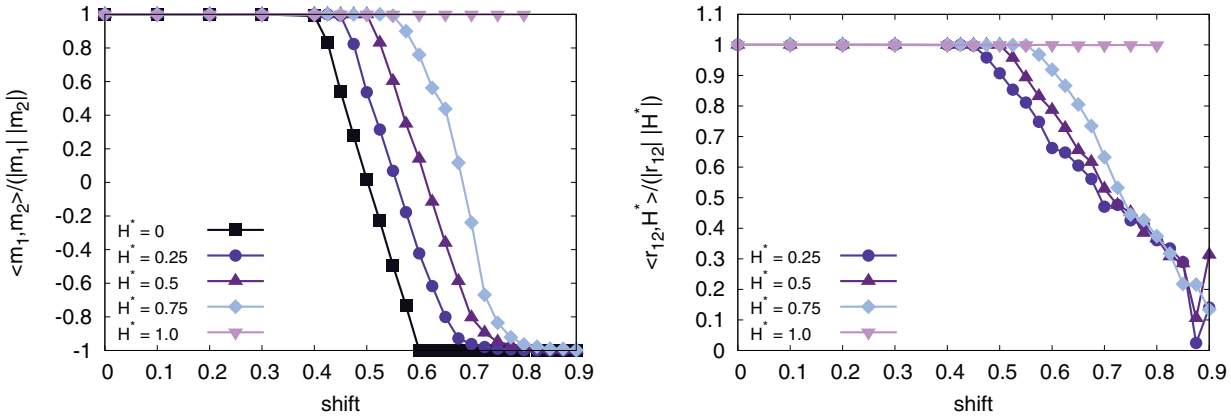

FIG. 2. (Left) Dot product between the magnetic moments of two particles in the ground state versus the shift for values of $H^* = 0 \ldots 1$. (Right) Dot product between the vector connecting the particles' centers and the external magnetic field for $H^* = 0.25 \ldots 1$. When the external field is increased, the transition from the head-to-tail dipole alignment to the anti-parallel one is moved towards higher shifts. At the same time, the cluster rotates such that the axis connecting the particles' centers is aligned perpendicular to the field. Once the dipole moments have reached the anti-parallel configuration, the ground states becomes degenerate, with respect to $\langle r_{12}, H \rangle$. Therefore, jumps in the curves appear. For $H^* \geq 1$, no transition occurs and the dipoles stay in the head-to-tail configuration at all shifts.

in Fig. 2, as well as the dot product of the vector connecting the particles' centers and the external field. In the left-hand side of Fig. 3, the dot products between the external field and the individual magnetic moments is plotted. On the right-hand side, all dot products are summarized for an external field of $H^* = 0.25$. It can be seen that the transition, described above, occurs for higher shifts, when the external field is stronger. This is the case, because a strong external field reinforces the head-to-tail configuration. We also find that both magnetic moments assume a roughly equal component parallel to the external field in the transition region. Only at very high shifts, the dipoles align anti-parallel in order to minimize the dipole-dipole interaction. At this point, one dipole moment has a component anti-parallel to the external field. Finally, we observe that, at $H^* = 1$, no transition occurs and the dipoles stay in the head-to-tail configuration at all shifts. In Fig. 4, the dimensionless energy for the dipole-dipole interaction (left) and dipole-field interaction (right) are compared. Both energies are normalized to their respective minimum values, $U_{dd}^{min} < 0$ and $U_{mf}^{min} < 0$. (Both of these minimum values are independent of the shift due to the scaling relations explained at the end of Sec. II). Due to the normalization by the minimum, which is smaller than zero, a larger ratio denotes a more favorable contribution to the energy. The plots of the normalized energy help to understand the competition between favoring the dipole-dipole interaction, and thus choosing an anti-parallel dipole alignment, or favoring the Zeeman energy, keeping the dipole moments parallel to the external field. For low shifts, the dipoles assume the head-to-tail configuration. Hence, the dipole-dipole energy can be optimized at the same time as the Zeeman energy. When the shift increases, the normalized dipole-dipole energy becomes more unfavorable, because the external field prevents the formation of an anti-parallel dipole alignment. The normalized Zeeman

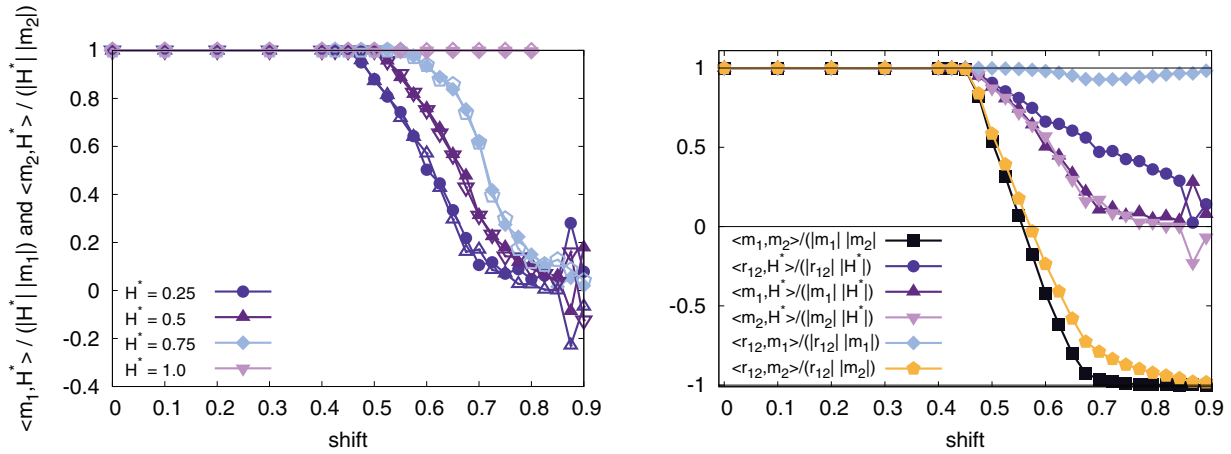

FIG. 3. (Left) Dot product between the external field and the first and second magnetic moments, respectively. The closed symbols indicate the moment of the first, the open symbols those of the second particle. (Right) Summary of all dot products for an external field of $H^* = 0.25$. In the transition region, where the dipole moments change from the head-to-tail to the anti-parallel configuration, the dipole moments rotate towards each other and thereby keep a component parallel to the external field to minimize the Zeeman energy. Only at very high shifts, one of the dipoles takes up a component anti-parallel to the field. This allows for an anti-parallel dipole alignment which is the most favorable at very high shifts.

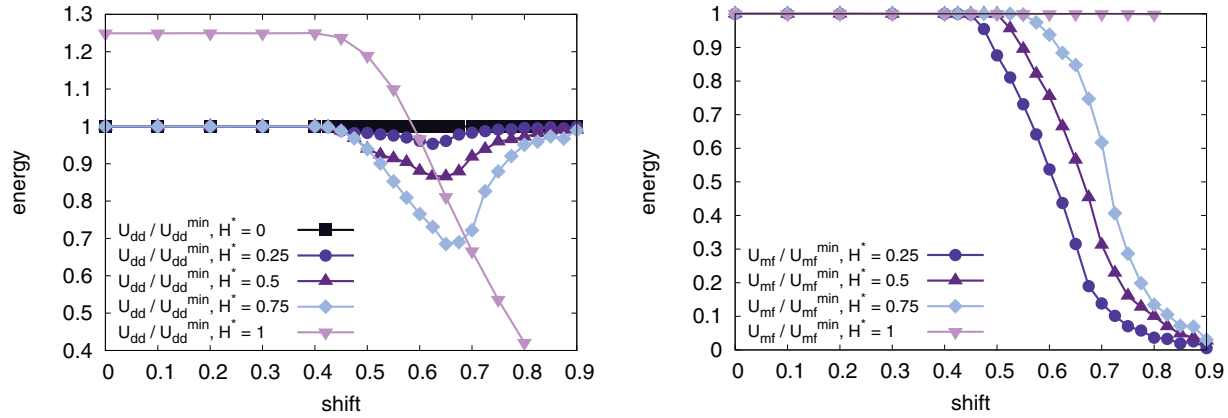

FIG. 4. Ratio of the energy of the dipole-dipole interaction (left) and the dipole-field interaction (right) to their respective minimal values, in the ground states of clusters of two SD-particles. As the energy values are normalized by their values at the global minima, which are negative, higher values of the ratio signify a more favorable configuration. When, at low shifts, the dipoles are oriented head-to-tail, both the dipole-dipole energy and the dipole-field energy reach their optimal (minimal) values. At higher shifts, the dipole-dipole energy shows a drop, as the external field prevents the dipoles from assuming the anti-parallel configuration which would be energetically most favorable. At very high shift, the advantage of arranging in an anti-parallel configuration is so large that the dipole-dipole energy increases again, but the dipole-field energy drops sharply.

energy also decreases, as a compromise is found between a favorable dipole alignment and an alignment of the dipoles with respect to the field. At very high shifts, the dipoles orient anti-parallel and optimize the dipole-dipole energy. At this point, the Zeeman energy approaches zero, as the contributions from the two dipoles compensate each other.

In summary, particles with central dipoles can orient their dipoles favorably towards each other and towards an external field at the same time. For SD-particles with a high shift, on the other hand, a favorable alignment for the dipole-dipole interaction contradicts a favorable alignment to the field. It will be seen in Sec. IV that this leads to a reduced clustering of SD-particles in an external field.

IV. SUSPENSIONS AT FINITE TEMPERATURE IN A MAGNETIC FIELD

In this section, the cluster structure and magnetization properties of a suspension of SD-particles at $k_BT > 0$ under the application of an external field are discussed.

A. Simulation technique

The suspensions at finite temperature were obtained by means of molecular dynamics simulations using the ESPResSo software package.[79,80] The simulations consist of $N = 1000$ particles. The volume fraction

$$\phi = N\frac{\pi d^3}{6l^3} \tag{10}$$

is set by changing the box size l. Periodic boundary conditions are employed to mimic bulk behavior. The dipole-dipole interaction was calculated using the dipolar P^3M algorithm.[81]

The temperature was kept constant by a Langevin thermostat.[82] By adding a velocity dependent friction and adding random kicks to the particles, it describes the drag force and the Brownian motion created by the carrier fluid. Thus, the equation of motion for a particle in one component is

$$m\ddot{x}_i = F_i - \gamma\dot{x}_i + F_{random}, \tag{11}$$

where γ is the friction constant, F_i denotes the force on particle i due to interactions with other particles, and F_{random} is a random force. This force is Gaussian distributed with a mean of zero and a variance of

$$\left\langle F_{random}^2 \right\rangle = 2\gamma k_B T. \tag{12}$$

A similar equation of motion is used for the rotational degrees of freedom. In our simulations, the friction constant γ, the thermal energy k_BT as well as the mass and the inertial moment are all set to unity. The shifted dipoles are implemented using the concept of virtual sites. These are particles, the position and orientation of which is not obtained by integrating Newton's equation of motion. Instead, these properties are derived from the position and orientation of other particles. In this way, a virtual site carrying a dipole moment is placed relative to the centre of mass of each SD-particle. After the forces and torques on the virtual site are calculated from the dipole-dipole interaction, they are transferred back to the centre of mass of the SD-particle. Then, the SD-particle's centre of mass is propagated using Newton's equations. Details can be found in Refs. 80 and 83.

Before sampling, the system is warmed up for 500 000 time steps of size $dt = 0.001$. Then, snapshots for cluster analysis are recorded 200 times with a spacing of 10 000 time steps, whereas the magnetization is measured every 100 time steps.

B. Structure of the suspension

In order to quantify the properties of the microstructure of a suspension of SD-particles in an external magnetic field, we perform a cluster analysis. It is based on a distance and energy criterion: neighboring particles are considered to be in the same cluster, if their centres are closer than 1.3 diameters,

and the dipolar interaction energy is negative. The algorithm is based on the Hoshen-Kopelman scheme.[84] Technical details are explained in Ref. 74. It is important to note that, in this paper, we include single particles in the cluster definition. This makes the average cluster size

$$S = \frac{1}{N_{clusters}} \sum_{i=1}^{\infty} i \cdot n_i \tag{13}$$

more meaningful at high shifts, when the system contains mostly pairs and single particles, but the ratio of these two still changes with the shift. In the equation, n_i refers to the number of clusters of size i.

It will be shown in Sec. IV C that the magnetic response of the system is mainly governed by the dipole moment per cluster and by the cluster size distribution. Hence, results for these will be presented below.

In Fig. 5 we show the distribution of the dipole moment M_c per cluster, i.e., $P(M_c)$. Here, M_c is normalized to the dipole moment of a single particle at the specified λ^* and s. Thus, a value of $M_c = 1$ indicates that the cluster has a magnetic moment with a magnitude of a single magnetic particle.

In the plot distributions for several shifts are compared. Let us first look at the interval $0 \leq M_c < 1$. All clusters of more than one particle can contribute to this region. When the shift is small, however, clusters tend to have a chain-like structure with head-to-tail dipole orientation. It is therefore very unlikely that such a cluster has a small total dipole moment. This can also be seen from the sharp drop by more than two orders of magnitude in the dipole moment distribution for $M_c < 1$. When the shift is high the dominant cluster structures are pairs and triangles with anti-parallel and ring-like dipole alignment. In these clusters, the dipole moments partially cancel out, so that the total dipole moment of the cluster typically is below $M_c = 1$. Hence, we observe a more flat distribution in the range $M_c < 1$.

At $M_c = 1$, we observe a strong peak originating from the single particles. For $M_c > n$, where n is the number of particles in the cluster, clusters of n particles can no longer contribute to the distribution. This is simply, because they cannot reach this value of M_c, even if all dipole moments in the cluster are co-aligned. This is the reason for the steps in the distribution at integer values of M_c, especially at $M_c = 2$. For higher values of M_c, we observe a long and smooth decay of the distribution for low shifts and a rather steep descend for high ones, as the long chains become very flexible and the total dipole moment is very broadly distributed. At high shifts, on the other hand, not many large clusters exist in the first place, and if they do exist, the dipoles in them tend to assume anti-parallel or ring-like dipole alignments, so that the cluster dipole moment is rather small.

In Fig. 6, the distribution of dipole moments per cluster is shown for a fixed shift of $s = 0.65$ for various applied magnetic fields. This helps to understand the change in cluster structure, as an external field is applied. For zero field, one again observes a significant number of clusters with normalized dipole moments smaller than $M_c = 1$. When an external field is applied this changes drastically. A field of $\alpha = 2$, causes the distribution to drop by roughly an order of magnitude at $M_c = 0$. This indicates a strong change in cluster structure: in an external field the ring-like and antiparallel dipole arrangements resulting in clusters with low dipole moments, become unfavorable. Due to the field, chain-like cluster structures with higher total dipole moments are more favorable. For high shifts, the distance between the dipoles is much larger in the co-aligned configuration than in ring-like and anti-parallel states. This leads to a weakening of the interactions between particles, when an external field forces them into chain-like configurations. For some cases, this leads to a reduction in cluster size, when an external field is applied. This will be examined in more detail in the following paragraph.

A plot of the cluster size at zero external field can be found in Ref. 74. The cluster size versus the shift first shows a small increase for shifts up to approximately 0.5. For even higher shifts it drops sharply until, at shifts around 0.8, mostly single particles and anti-parallel pairs are found.

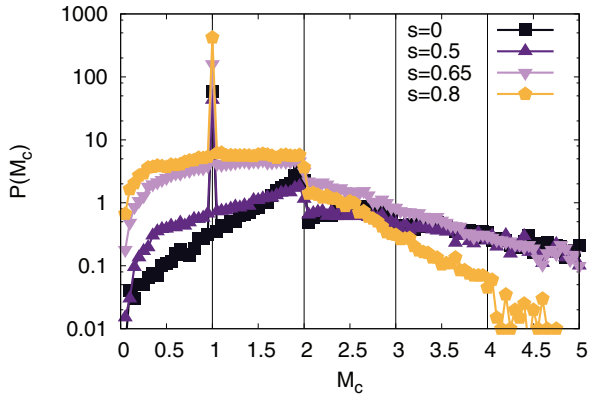

FIG. 5. Distribution of dipole moments per cluster at zero external field for $\lambda^* = 4$, $\phi = 0.09$, and various shifts. For zero shift, only very few clusters have a dipole moment below that of a single particle. For a higher shift, the probability for clusters showing a dipole moment below that of a single particle increases by up to two orders of magnitude, as a significant number of clusters have anti-parallel or triangular dipole arrangements. At high shifts, this dipole moment distribution almost entirely controls the initial susceptibility, as will be shown in Sec. IV C.

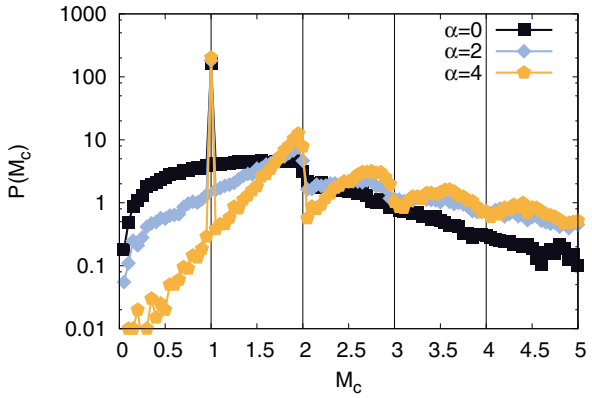

FIG. 6. Distribution of dipole moment per cluster at a shift of $s = 0.65$ and $\lambda^* = 4$ for various fields ($\phi = 0.09$). It can be seen that the number of clusters with dipole moments less than that of a single particle drops sharply, when an external field is applied.

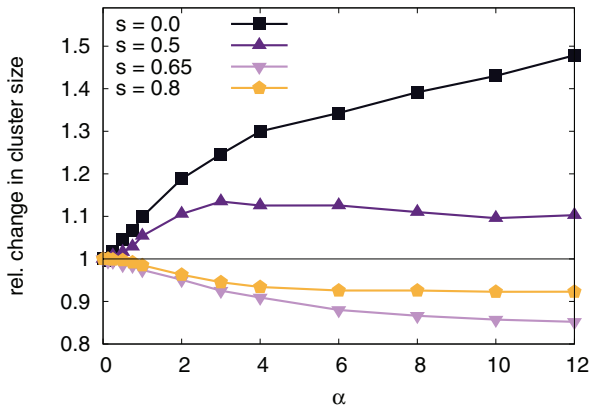

FIG. 7. Relative change in cluster size versus the applied field ($\phi = 0.06$). For zero shift, the average cluster size grows in an applied field, as the field enhances the formation of chains. This effect is dampened with increasing shift, as chains are no longer the preferred configuration of the SD-particles. At very high shifts, the cluster size even decreases when the field is applied, presumably due to the destruction of clusters with anti-parallel or ring-like dipole arrangements.

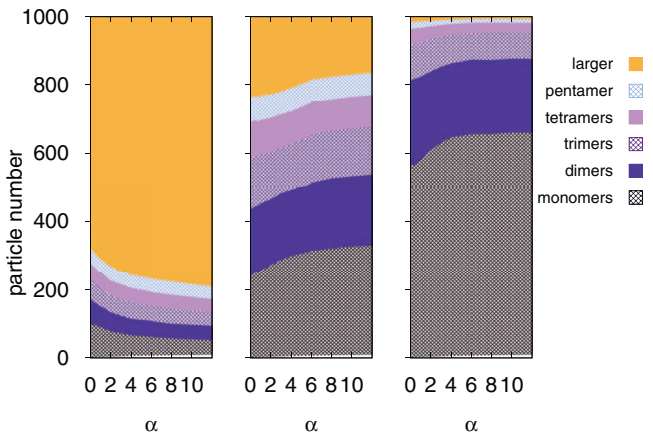

FIG. 8. Distribution of cluster sizes versus the field for shifts $s = 0$, $s = 0.65$, and $s = 0.8$. The width of the stripe indicates the fraction of the system consisting of the respective cluster type. For zero shifts, the number of small clusters falls sharply when a field is applied. When the shift is increased, the number of large clusters decreases. When the shift is high, we observe an increase of single particles and smaller clusters in an external field.

In Fig. 7, the relative change in cluster size is shown versus the field strength given for several shifts for the interaction parameter $\lambda^* = 4$. The relative change was chosen, because the absolute change in cluster size varies strongly for different shifts. For small s, the clusters grow strongly when an external field is applied. This is, because the formation of long chains of particles is even more probable, if all dipoles are aligned to roughly the same direction by the external field. However, the cluster growth is reduced significantly for increasing shifts, and the clusters shrink by approximately 5% for $s = 0.8$ and approximately 15% for $s = 0.65$.

In Fig. 8, we take a closer look at the change in composition of the suspension, when a magnetic field is applied. To this end, the fraction of the system consisting of clusters of different sizes is indicated by the width of the stripes. Results are shown for shifts of $s = 0$, $s = 0.65$, and $s = 0.8$, and the value of $\lambda^* = 4$. The basic trends are comparable to those observed for the relative change in cluster size in Fig. 7: For zero shift, the number of particles in small clusters and, in particular, the number of single particles drops significantly, when even a small field is applied. This changes, when the shift is higher, and clusters with anti-parallel and ring-like dipole alignment become more dominant. The number of larger clusters decreases when a field is applied. The reduction of cluster size and a change in composition towards smaller clusters in an applied magnetic field is unusual and opposite to what is observed for particles with central dipoles. For visual purposes, we show snapshots of the simulation box for a shift of $s = 0$ and 0.725 in Fig. 9. We present snapshots for both, the field free case ($\alpha = 0$) and an applied field of large field strength pointing to the right ($\alpha = 12$). What can be clearly seen by eye is that in the case of central dipoles, the application of an external field leads to strong chain formation in the suspension. When the dipole moments are shifted towards the particles' surface, the dipoles are still aligned to the field but no chains form. At the same time, small clusters with anti-parallel dipole alignment are broken up by the external field, corroborating our more detailed analysis presented before.

C. Magnetic properties

The magnetization curve describes the total dipole moment of a ferrofluid versus the applied external field. Thus, the magnetization is the sum of all dipoles in the system:

$$M = \sum_i \vec{m}_i. \tag{14}$$

For non-interacting dipoles, the magnetization curve follows a Langevin law given by

$$\frac{M}{M_{sat}} = \coth\alpha - \frac{1}{\alpha}, \tag{15}$$

where the so-called Langevin parameter is given by Eq. (8). It has been shown[18] that, for spherical particles with central dipoles, the magnetization is always greater or equal to the one given by the Langevin law. This can be rationalized by the fact that each particle aligns its moment along the external field, but this process is enhanced due the local field emanating from the neighboring aligned particles.

On the left-hand side of Fig. 10, the magnetization curves are shown for various shifts for a suspension with volume fraction $\phi = 0.03$. The plot on the right-hand side shows the difference between the magnetization and the Langevin law (Eq. (15)). The dipolar interaction parameter is $\lambda^* = 4$ in both cases. At zero field, all systems show no net magnetic moment. At very strong fields, all dipoles are aligned and the magnetization approaches its saturation value. However, in the medium range of fields, the magnetization strongly depends on the shift: for low shifts, the magnetization is significantly higher than the value expected for non-interacting dipoles. This is in accordance with the mean field[18] and density functional theory[8,21,32] results for particles with central dipoles. When the shift is increased, the magnetization of the

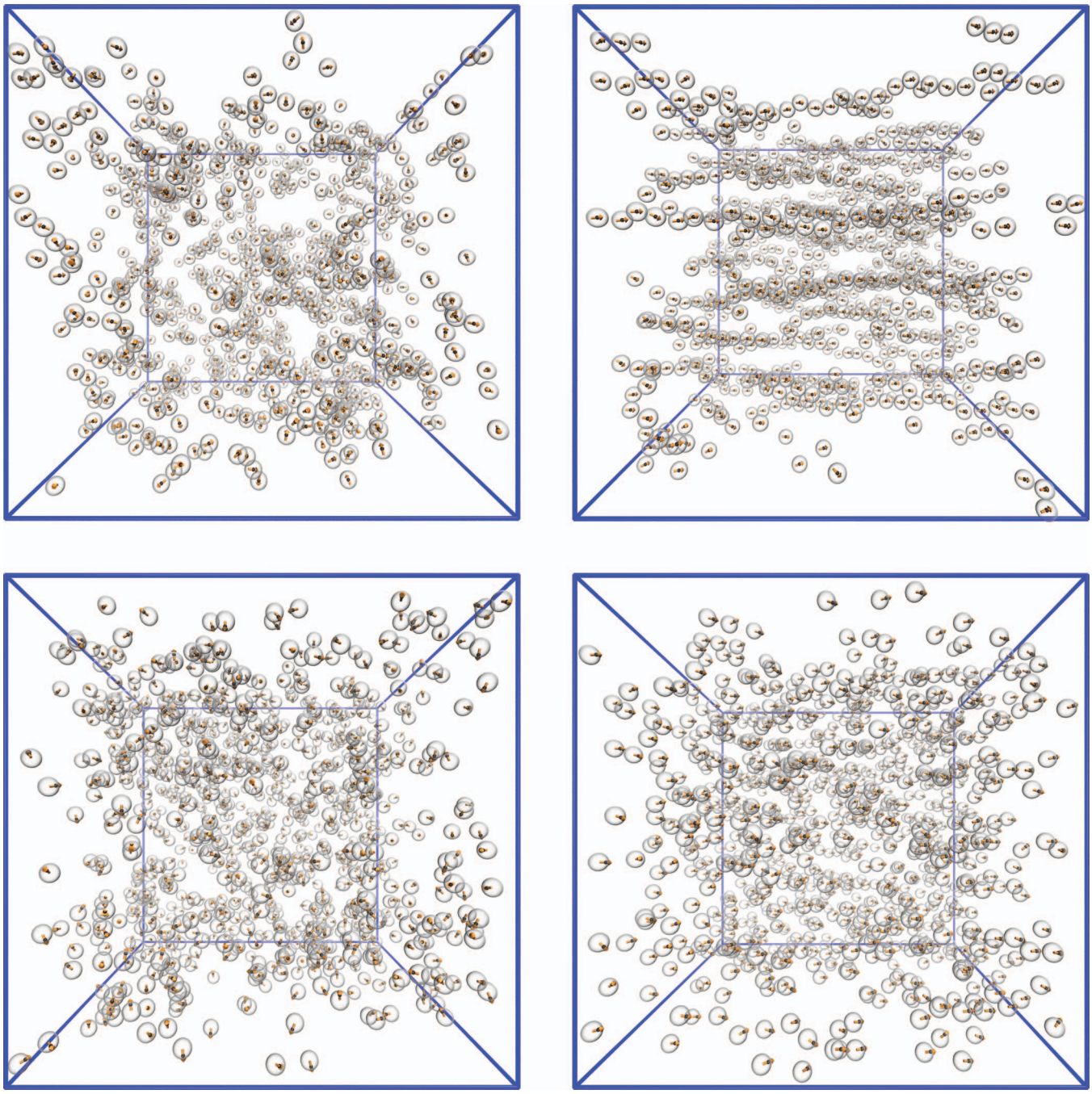

FIG. 9. Snapshots of suspensions of SD-particles at shift $s = 0$ (top) and $s = 0.725$ (bottom) for no external magnetic field (left) and a field pointing to the right of strength $\alpha = 12$ (right). It can be seen that, in the case of central dipoles, the application of an external field leads to strong chain formation in the suspension. When the dipole moments are shifted towards the particles' surface, the dipoles are still aligned to the field but no chains form. At the same time, small clusters with anti-parallel dipole alignment are broken apart by the external field. (Rendered with vmd.[85])

suspension decreases. This is driven by two effects: first, as shown in Ref. 74, the cluster size decreases for higher shift. As particles are further apart, they do not extend each other's magnetization to a similar degree. Second, at high shift, the dipoles of neighboring particles assume ring-like or even anti-parallel alignments, which means that some of the dipoles in a cluster assume a non-favorable alignment with respect to the magnetic field. When an external field is applied, the binding energy of the ring-like or anti-parallel dipole structure competes with the loss of Zeeman energy. This leads to a magnetization which is even below the Langevin value for suspensions with strong dipolar interaction and medium to high shift. Only when the field is stronger, the clusters get broken up, as the magnetic particles get aligned by the field. In some cases, this leads to a decrease of cluster size versus the applied field as shown in Fig. 7. This is quite opposite to what is observed in suspensions with central dipoles.[8,21]

In addition to the complete magnetization curves, it is helpful to study the initial susceptibility, i.e., the slope of the magnetization curve in the limit of zero external field. This will allow for a quantitative comparison of the dependency of the low-field magnetization behavior on parameters like the

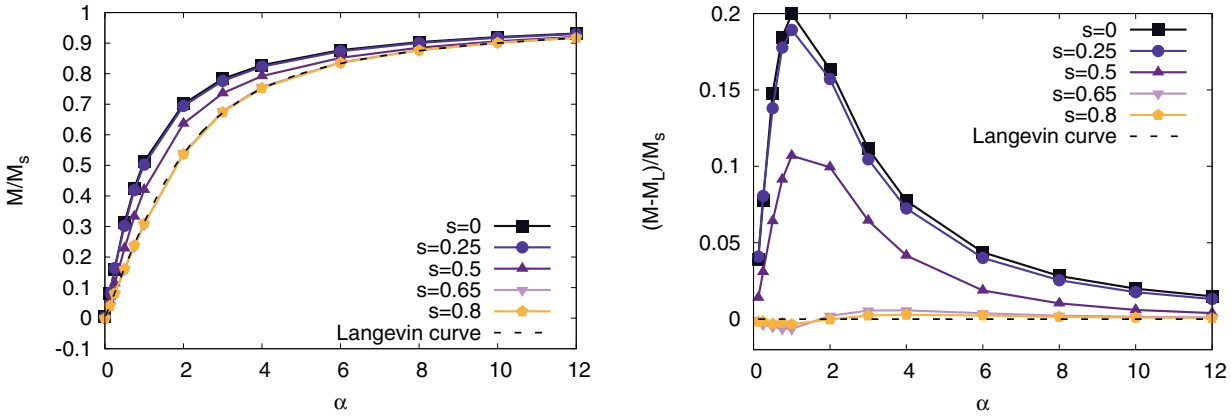

FIG. 10. Magnetization curves (left) and difference between observed magnetization curve and that for non-interacting dipoles (right) for a volume fraction of $\phi = 0.03$. The dipolar interaction parameter is $\lambda^* = 4$. It can be seen that the magnetization curve is significantly above the Langevin curve for zero shift. It falls back toward the Langevin curve for higher shifts, as the cluster size decreases and neighboring particles tend to have more anti-parallel orientations. For some configurations, the magnetization curve even falls below the Langevin law. Note that on the left-hand side, the curves for $s = 0.65$ and $s = 0.8$ coincide. Small differences can be observed on the right-hand side.

shift. In computer simulations, the initial susceptibility can be obtained either from a linear fit to the magnetization curve, or, typically more accurately, from the fluctuation of the system's total magnetic moment at zero external field.[86] Here we employ the latter approach. The fluctuation formula for the susceptibility for metallic Ewald boundary conditions at infinity is given by

$$\chi = \frac{\phi \langle M^2 \rangle}{4\pi r^3 N}, \tag{16}$$

where M is the total dipole moment of the system. In contrast to Ref. 86, this is written in terms of the volume fraction ϕ rather than the number density. In Fig. 11, the initial susceptibility is shown for volume fractions between 0.03 and 0.09 and dipolar interaction parameters of $\lambda^* = 3$ and $\lambda^* = 4$. It can be seen that the susceptibility drops by a factor of approximately three when the shift is increased. For strong interaction parameters, the initial susceptibility falls below the

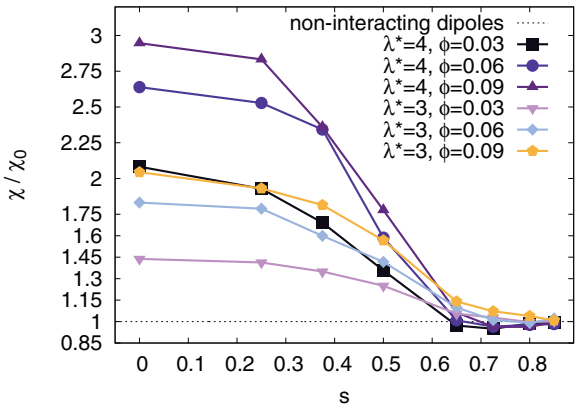

FIG. 11. Initial susceptibility versus the shift s at $\phi = 0.03$ to $\phi = 0.09$. The dipolar interaction parameters are $\lambda^* = 3$ and 4. The results are normalized to the susceptibility of non-interacting dipoles with the same dipole moment. The reduction of susceptibility solely due to the scaling of λ^* is not shown. It can be seen that, for small shifts, the susceptibility is significantly larger than the value for non-interacting dipoles. For shifts around $s = 0.65$, on the other hand, the susceptibility is below the Langevin susceptibility, as clusters with anti-parallel or triangular dipole configuration hinder the magnetization.

Langevin susceptibility at a shift of approximately 0.65. For even higher shift, the susceptibility approaches the Langevin value from below. This behavior can be understood by noting that at small shifts neighboring particles' dipoles are co-aligned and hence, the magnetization is enhanced. When the shift increases, the cluster size drops and particles become evenly distributed over the entire system. Therefore, the susceptibility drops towards the case for non-interacting dipoles. Additionally, the clusters that still do exist at higher shifts tend to have ring-like or anti-parallel dipole alignments. This, as explained above, hinders the magnetization and leads to a susceptibility that even is below the Langevin value. It should be noted that the Langevin susceptibility is understood in terms of the shift-adjusted dipole moment $m(s)$ (Eq. (6)). If one were not doing this scaling, the drop in susceptibility would be dominated by the effect of the scaling, and results for different shifts would not be comparable.

Let us now explore further, how much the susceptibility is influenced by the cluster structure of the suspension. To this end, we compare the full susceptibility as obtained by Eq. (16), to the susceptibility obtained for non-interacting, rigid clusters. To this end, a cluster analysis of the suspension is performed and the total magnetic moment of each cluster is determined. Then, it is assumed that the magnitude of the magnetic moment of the cluster stays constant for very small external fields, and that the clusters do not interact among each other. The susceptibility of this system is given by

$$\chi_c = \frac{1}{3V\mu_0 k_B T} \left\langle \sum_i m_i^2 \right\rangle, \tag{17}$$

where i iterates over all clusters including single particles, V denotes the volume, and m_i denotes the magnetic moment of each cluster. In Fig. 12, the susceptibilities for the full system and for the system of rigid, non-interacting clusters are compared. It can be observed that for low shifts, the susceptibility for the full system is much higher than that of the fictitious system: clusters found at low shifts are mainly chain-like, and show a head-to-tail dipole alignment. Hence, there is a strong interaction between clusters, which cannot be ignored

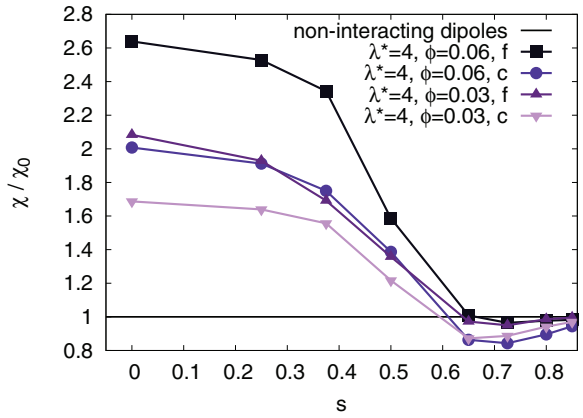

FIG. 12. Full susceptibility compared to the susceptibility obtained under the assumption of non-interacting clusters. It can be seen that the susceptibility at low shift is strongly influenced by correlations between clusters. Hence, the full susceptibility is higher than that for the approximation of non-interacting, rigid clusters. On the other hand, the susceptibility is almost entirely dominated by individual clusters at high shifts, in particular in the region where the susceptibility is below the Langevin susceptibility.

when determining properties of the system. When the shift becomes large, in particular, when the susceptibility drops below the Langevin value at $s \approx 0.7$, the susceptibilities for the two systems are similar in magnitude. At these shift values, the clusters have ring-like or anti-parallel dipole alignments and a very small dipole moment, as the dipoles of neighboring particles partially cancel out. Therefore, the interaction between clusters, which roughly depends on the product of the clusters' magnetic moments, becomes mostly negligible. In particular, the susceptibility below the Langevin value can be found even in the approximation of non-interacting, rigid clusters.

V. SUMMARY

We presented a detailed study of a SD-particle system under the influence of an external field. For particles with central dipoles, the two-particle ground states are the usual head-to-tail configuration. It allows for the magnetic particles to maximize the absolute value of the dipole-dipole interaction and the dipole-field interaction at the same time. This is, in general, no longer the case for particles with shifted dipoles. In a field, either the dipoles align favorably to each other, i.e., more and more anti-parallel, when the shift is increased, or they align to the external field. This competition is also observed for suspensions at finite temperatures. In that case, we observe a strong reduction in clusters with magnetic moments smaller than that of a single particle, when a field is applied. In contrast to suspensions of particles with central dipoles, a reduction of cluster size with increasing field is observed for some parameters. This has also been observed in an experimental realisation where the effect can be exploited for a reversible self-assembly process.[71] The competition between anti-parallel and ring-like dipole alignments in clusters of SD-particles and an external field also leads to a hindered magnetization behavior. The initial susceptibility can fall below the Langevin value for non-interacting dipoles depending on the chosen parameters. This is a very surprising and unusual behavior for magnetic soft matter.

ACKNOWLEDGMENTS

R.W. and C.H. are grateful for financial support from the SRC SimTech, and for access to the computer facilities of the HLRS. S.K. was supported by Austrian Science Fund (FWF): START-Project Y 627-N27, RFBR Grant Nos. mol-a 1202-31-374 and mol-a-ved 12-02-33106, and the Grant of Ministry of Science and Education of RF 2.609.2011. The authors are grateful to Dr. J. J. Cerda for discussions in the initial stage of this work, and to Dr. M. Sega, Dr. O. Lenz, F. Fahrenberger, and G. Rempfer for help with some figures.

[1] L. Resler, Jr. and R. E. Rosensweig, "Magnetocaloric power," AIAA J. **2**, 1418–1422 (1964).
[2] Y. N. Skibin, V. V. Chekanov, and Y. L. Raikher, "Birefringence in a ferromagnetic liquid," J. Exp. Theor. Phys. **45**(3), 496–499 (1977).
[3] P. C. Scholten, "The origin of magnetic birefringence and dichroism in magnetic fluids," IEEE Trans. Magn. **16**, 221–225 (1980).
[4] S. Taketomi, "Magnetic fluids anomalous pseudo-cotton mouton effects about 10^7 larger than that of nitrobenzene," Jpn. J. Appl. Phys. **22**, 1137–1143 (1983).
[5] M. Holmes, K. O'Grady, and J. Popplewell, "A study of curie-weiss behaviour in ferrofluids," J. Magn. Magn. Mater. **85**(1–3), 47–50 (1990).
[6] V. M. Buzmakov and A. F. Pshenichnikov, "On the structure of microaggregates in magnetite colloids," J. Colloid Interface Sci. **182**, 63–70 (1996).
[7] S. Odenbach, *Magnetoviscous Effects in Ferrofluids*, Lecture Notes in Physics Vol. 71 (Springer, Berlin, 2002).
[8] M. Klokkenburg, B. H. Erné, V. Mendelev, and A. O. Ivanov, "Magnetization behavior of ferrofluids with cryogenically imaged dipolar chains," J. Phys.: Condens. Matter **20**(20), 204113–204117 (2008).
[9] A. V. Lebedev, "Low-temperature magnetic fluid stabilized with mixed fatty acids," Colloid J. **72**(6), 815–819 (2010).
[10] A. V. Lebedev and S. N. Lysenko, "Magnetic fluids stabilized by polypropylene glycol," J. Magn. Magn. Mater. **323**(10), 1198–1202 (2011).
[11] K. I. Morozov, A. F. Pshenichnikov, Y. L. Raikher, and M. I. Shliomis, "Magnetic properties of ferrocolloids: The effect of interparticle interactions," J. Magn. Magn. Mater. **65**, 269–272 (1987).
[12] M. I. Shliomis, A. F. Pshenichnikov, K. I. Morozov, and I. Yu. Shurubor, "Magnetic properties of ferrocolloids," J. Magn. Magn. Mater. **85**(1–3), 40–46 (1990).
[13] Y. A. Buyevich and A. O. Ivanov, "Equilibrium properties of ferrofluids," Physica A **190**, 276 (1992).
[14] A. Yu. Zubarev and L. Yu. Iskakova, "Theory of physical properties of magnetic liquids with chain aggregates," J. Exp. Theor. Phys. **80**, 857 (1995).
[15] M. A. Osipov, P. I. C. Teixeira, and M. M. TelodaGama, "Structure of strongly dipolar fluids at low densities," Phys. Rev. E **54**(3), 2597 (1996).
[16] B. Huke and M. Lücke, "Magnetization of ferrofluids with dipolar interactions: A born-mayer expansion," Phys. Rev. E **62**(5), 6875–6890 (2000).
[17] B. Huke and M. Lücke, "Cluster expansion for ferrofluids and the influence of polydispersity on magnetization," J. Magn. Magn. Mater. **252**, 132–134 (2002).
[18] A. O. Ivanov and O. B. Kuznetsova, "Magnetic properties of dense ferrofluids: an influence of interparticle correlations," Phys. Rev. E **64**, 041405 (2001).
[19] S. Kantorovich and A. O. Ivanov, "Formation of chain aggregates in magnetic fluids: an influence of polydispersity," J. Magn. Magn. Mater. **252**, 244–246 (2002).
[20] A. O. Ivanov and S. S. Kantorovich, "Chain aggregate structure and magnetic birefringence in polydisperse ferrofluids," Phys. Rev. E **70**, 021401 (2004).
[21] A. O. Ivanov, S. S. Kantorovich, V. S. Mendelev, and E. S. Pyanzina, "Ferrofluid aggregation in chains under the influence of a magnetic field," J. Magn. Magn. Mater. **300**, e206–e209 (2006).
[22] E. A. Elfimova, A. O. Ivanov, and P. J. Camp, "Theory and simulation of anisotropic pair correlations in ferrofluids in magnetic fields," J. Chem. Phys. **136**(19), 194502 (2012).

[23]S. Kantorovich, A. O. Ivanov, L. Rovigatti, J. Maria Tavares, and F. Sciortino, "Nonmonotonic magnetic susceptibility of dipolar hard-spheres at low temperature and density," Phys. Rev. Lett. **110**, 148306 (2013).
[24]J. J. Weis and D. Levesque, "Chain formation in low density dipolar hard spheres: a monte carlo study," Phys. Rev. Lett. **71**(17), 2729–2732 (1993).
[25]J. J. Weis and D. Levesque, "Ferroelectric phases of dipolar hard shperes," Phys. Rev. E **48**(5), 3728–3740 (1993).
[26]P. J. Camp, J. C. Shelley, and G. N. Patey, "Isotropic fluid phases of dipolar hard spheres," Phys. Rev. Lett. **84**(1), 115–118 (2000).
[27]Z. Wang and C. Holm, "Structure and magnetization properties of polydispersed ferrofluids: A molecular dynamics study," Phys. Rev. E **68**, 041401 (2003).
[28]T. Kristóf and I. Szalai, "Magnetic properties and structure of polydisperse ferrofluid models," Phys. Rev. E **68**(4), 041109 (2003).
[29]J. P. Huang and C. Holm, "Magnetization of polydisperse colloidal ferrofluids: Effect of magnetostriction," Phys. Rev. E **70**, 061404 (2004).
[30]C. Holm and J.-J. Weis, "The structure of ferrofluids: A status report," Curr. Opin. Colloid Interface Sci **10**, 133–140 (2005).
[31]A.-P. Hynninen and M. Dijkstra, "Phase diagram of dipolar hard and soft spheres: Manipulation of colloidal crystal structures by an external field," Phys. Rev. Lett. **94**, 138303 (2005).
[32]C. Holm, A. Ivanov, S. Kantorovich, E. Pyanzina, and E. Reznikov, "Equilibrium properties of a bidisperse ferrofluid with chain aggregates: theory and computer simulations," J. Phys.: Condens. Matter **18**, S2737–S2756 (2006).
[33]J. Jordanovic and S. H. L. Klapp, "Field-induced layer formation in dipolar nanofilms," Phys. Rev. Lett. **101**, 038302 (2008).
[34]J. Richardi and J.-J. Weis, "Low density mesostructures of confined dipolar particles in an external field," J. Chem. Phys. **135**(12), 124502 (2011).
[35]V. A. Danilov, T. A. Prokopieva, and S. Kantorovich, "Ground state structures and structural transitions in a monolayer of magnetic dipolar particles in the presence of an external magnetic field," Phys. Rev. E **86**, 061408 (2012).
[36]P. Langevin, "Magnetisme et theorie des electrons," Ann. Chim. Phys. **5**, 70 (1905).
[37]S. Odenbach and H. Gilly, "Taylor vortex flow of magnetic fluids under the influence of an azimuthal magnetic field," J. Magn. Magn. Mater. **152**, 123 (1996).
[38]S. Odenbach and S. Thurm, "Magnetoviscous effects in ferrofluids," *Ferrofluids: Magnetically Controllable Fluids and Their Applications*, Lecture Notes in Physics Vol. 594, edited by S. Odenbach (Springer, Berlin, Germany, 2002), pp. 185–201.
[39]S. Odenbach, "Recent progress in magnetic fluid research," J. Phys.: Condens. Matter **16**(32), R1135 (2004).
[40]P. Ilg, E. Coquelle, and S. Hess, "Structure and rheology of ferrofluids: simulation results and kinetic models," J. Phys.: Condens. Matter **18**(38, Sp. Iss. SI), S2757–S2770 (2006).
[41]S. Mahle, P. Ilg, and M. Liu, "Hydrodynamic theory of polydisperse chain-forming ferrofluids," Phys. Rev. E **77**, 016305 (2008).
[42]E. Hasmonay, J. Depeyrot, M. H. Sousa, F. A. Tourinho, J. C. Bacri, R. Perzynski, Y. L. Raikher, and I. Rosenman, "Magnetic and optical properties of ionic ferrofluids based on nickel ferrite nanoparticles," J. Appl. Phys. **88**, 6628–6635 (2000).
[43]Y. L. Raikher, V. I. Stepanov, J. Depeyrot, M. H. Sousa, F. A. Tourinho, E. Hasmonay, and R. Perzynski, "Dynamic optical probing of the magnetic anisotropy of nickel-ferrite nanoparticles," J. Appl. Phys. **96**(9), 5226–5233 (2004).
[44]D. Jamon, F. Donatini, A. Siblini, F. Royer, R. Perzynski, V. Cabuil, and S. Neveu, "Experimental investigation on the magneto-optic effects of ferrofluids via dynamic measurements," J. Magn. Magn. Mater. **321**(9), 1148–1154 (2009).
[45]G. Meriguet, E. Dubois, A. Bourdon, G. Demouchy, V. Dupuis, and R. Perzynski, "Forced rayleigh scattering experiments in concentrated magnetic fluids: effect of interparticle interactions on the diffusion coefficient," J. Magn. Magn. Mater. **289**, 39 (2005).
[46]P. J. Camp and G. N. Patey, "Structure and scattering in colloidal ferrofluids," Phys. Rev. E **62**(4), 5403–5408 (2000).
[47]L. M. Pop and S. Odenbach, "Investigation of the microscopic reason for the magnetoviscous effect in ferrofluids studied by small angle neutron scatting," J. Phys.: Condens. Matter **18**, S2785 (2006).
[48]D. Bica, L. Vekas, M. V. Avdeev, O. Marinica, V. Socoliuc, M. Balasoiu, and V. M. Garamus, "Sterically stabilized water based magnetic fluids: Synthesis, structure and properties," J. Magn. Magn. Mater. **311**, 17 (2007).
[49]A. Wiedenmann, U. Keiderling, M. Meissner, D. Wallacher, R. Gahler, R. P. May, S. Prevost, M. Klokkenburg, B. H. Erné, and J. Kohlbrecher, "Low-temperature dynamics of magnetic colloids studied by time-resolved small-angle neutron scattering," Phys. Rev. B **77**, 184417 (2008).
[50]J. J. Cerda, E. Elfimova, V. Ballenegger, E. Krutikova, A. Ivanov, and C. Holm, "Behavior of bulky ferrofluids in the diluted low-coupling regime: Theory and simulation," Phys. Rev. E **81**, 011501 (2010).
[51]M. V. Avdeev, E. Dubois, G. Mériguet, E. Wandersman, V. M. Garamus, A. V. Feoktystov, and R. Perzynski, "Small-angle neutron scattering analysis of a water-based magnetic fluid with charge stabilization: contrast variation and scattering of polarized neutrons," J. Appl. Crystallogr. **42**(6), 1009–1019 (2009).
[52]E. Pyanzina, S. Kantorovich, J. J. Cerda, A. Ivanov, and C. Holm, "How to analyse the structure factor in ferrofluids with strong magnetic interactions: a combined analytic and simulation approach," Mol. Phys. **107**, 571–590 (2009).
[53]A. Skumiel, T. Hornowski, and A. Jazefczak, "Investigation of magnetic fluids by ultrasonic and magnetic methods," Ultrasonics **38**(1–8), 864–867 (2000).
[54]A. S. Lubbe, C. Alexiou, and C. Bergemann, "Clinical applications of magnetic drug targeting," J. Surg. Res. **95**, 200–206 (2001).
[55]R. L. Snyder, V. Q. Nguyen, and R. V. Ramanujan, "Design parameters for magneto-elastic soft actuators," Smart Mater. Struct. **19**(5), 055017 (2010).
[56]R. Fuhrer, E. K. Athanassiou, N. A. Luechinger, and W. J. Stark, "Crosslinking metal nanoparticles into the polymer backbone of hydrogels enables preparation of soft, magnetic field-driven actuators with muscle-like flexibility," Small **5**(3), 383–388 (2009).
[57]D. Szabó, G. Szeghy, and M. Zrínyi, "Shape transition of magnetic field sensitive polymer gels," Macromolecules **31**, 6541–6548 (1998).
[58]B. Y. Ku, M.-L. Chan, Z. Ma, and D. A. Horsley, "Frequency-domain birefringence measurement of biological binding to magnetic nanoparticles," J. Magn. Magn. Mater. **320**(18), 2279–2283 (2008).
[59]L. V. Nikitin, D. G. Korolev, G. P. Stepanov, and L. S. Moronova, "Experimental study of magnetoelastics," J. Magn. Magn. Mater. **300**, e234 (2006).
[60]C. Gollwitzer, A. Turanov, M. Krekhova, G. Lattermann, I. Rehberg, and R. Richter, "Measuring the deformation of a ferrogel in a homogeneous magnetic field," J. Chem. Phys. **128**, 164709 (2008).
[61]G. Filipcsei, I. Csetneki, A. Szilágyi, and M. Zrínyi, "Magnetic field-responsive smart polymer composites," Adv. Polym. Sci. **206**, 137 (2007).
[62]R. Weeber, S. Kantorovich, and C. Holm, "Deformation mechanisms in 2d magnetic gels studied by computer simulations," Soft Matter **8**, 9923–9932 (2012).
[63]F. Vereda, J. de Vicente, and R. Hidalgo-Alvarez, "Physical properties of elongated magnetic particles: Magnetization and friction coefficient anisotropies," Chem. Phys. Chem. **10**(8), 1165 (2009).
[64]C. E. Alvarez and S. H. L. Klapp, "Percolation and orientational ordering in systems of magnetic nanorods," Soft Matter **8**, 7480–7489 (2012).
[65]A. P. Philipse, M. P. B. van Bruggen, and C. Pathmamanoharan, "Magnetic silica dispersions: preparation and stability of surface-modified silica particles with a magnetic core," Langmuir **10**, 92 (1994).
[66]G. Ganzenmueller and P. J. Camp, "Vapor-liquid coexistence in fluids of charged hard dumbbells," J. Chem. Phys. **126**, 191104 (2007).
[67]S. Lago, S. López-Vidal, B. Garzó, J. A. Mejías, J. A. Anta, and S. Calero, "Structure of liquids composed of shifted dipole linear molecules," Phys. Rev. E **68**, 021201 (2003).
[68]L. Baraban, D. Makarov, M. Albrecht, N. Rivier, P. Leiderer, and A. Erbe, "Frustration-induced magic number clusters of colloidal magnetic particles," Phys. Rev. E **77**, 031407 (2008).
[69]N. Mikuszeit, L. Baraban, E. Y. Vedmedenko, A. Erbe, P. Leiderer, and R. Wiesendanger, "Quasiantiferromagnetic 120° néel state in two-dimensional clusters of dipole-quadrupole-interacting particles on a hexagonal lattice," Phys. Rev. B **80**, 014402 (2009).
[70]J. Yan, M. Bloom, S. C. Bae, E. Luijten, and S. Granick, "Linking synchronization to self-assembly using magnetic janus colloids," Nature (London) **491**, 578 (2012).
[71]S. Sacanna, L. Rossi, and D. J. Pine, "Magnetic click colloidal assembly," J. Am. Chem. Soc. **134**(14), 6112–6115 (2012).
[72]S. Kantorovich, R. Weeber, J. J. Cerda, and C. Holm, "Ferrofluids with shifted dipoles: ground state structures," Soft Matter **7**(11), 5217–5227 (2011).
[73]S. Kantorovich, R. Weeber, J. J. Cerdà, and C. Holm, "Magnetic particles with shifted dipoles," J. Magn. Magn. Mater. **323**(10), 1269–1272 (2011).

[74]M. Klinkigt, R. Weeber, S. Kantorovich, and C. Holm, "Cluster formation in systems of shifted-dipole particles," Soft Matter **9**, 3535–3546 (2013).
[75]M. Piastra and E. G. Virga, "Phase polarity in a ferrofluid monolayer of shifted-dipole spheres," Soft Matter **8**, 10969 (2013).
[76]J. D. Weeks, D. Chandler, and H. C. Andersen, "Role of repulsive forces in determining the equilibrium structure of simple liquids," J. Chem. Phys. **54**, 5237 (1971).
[77]N. Metropolis, A. W. Rosenbluth, M. N. Rosenbluth, A. H. Teller, and E. Teller, "Equation of state calculations by fast computing machines," J. Chem. Phys. **21**(6), 1087 (1953). The original paper of the Metropolis algorithm.
[78]T. Prokopieva, V. Danilov, S. Kantorovich, and C. Holm, "Ground state structures in ferrofluid monolayers," Phys. Rev. E **80**(3), 031404 (2009).
[79]H. J. Limbach, A. Arnold, B. A. Mann, and C. Holm, "ESPResSo – An extensible simulation package for research on soft matter systems," Comput. Phys. Commun. **174**(9), 704–727 (2006).
[80]A. Arnold, O. Lenz, S. Kesselheim, R. Weeber, F. Fahrenberger, D. Roehm, P. Košovan, and C. Holm, "ESPResSo 3.1 — Molecular dynamics software for coarse-grained models," *Meshfree Methods for Partial Differential Equations VI*, Lecture Notes in Computational Science and Engineering, Vol. 89, edited by M. Griebel and M. A. Schweitzer (Springer, 2013), pp. 1–23.
[81]J. J. Cerdà, V. Ballenegger, O. Lenz, and C. Holm, "P3M algorithm for dipolar interactions," J. Chem. Phys. **129**, 234104 (2008).
[82]G. S. Grest and K. Kremer, "Molecular dynamics simulation for polymers in the presence of a heat bath," Phys. Rev. A **33**(5), 3628–3631 (1986).
[83]Z. Wang, C. Holm, and H. Walter Müller, "Molecular dynamics study on the equilibrium magnetization properties and structure of ferrofluids," Phys. Rev. E **66**, 021405 (2002).
[84]J. Hoshen and R. Kopelman, "Percolation and cluster distribution. I. cluster multiple labeling technique and critical concentration algorithm," Phys. Rev. B **14**, 3438–3445 (1976).
[85]W. Humphrey, A. Dalke, and K. Schulten, "VMD: Visual molecular dynamics," J. Mol. Graphics **14**, 33–38 (1996).
[86]Z. Wang, C. Holm, and H. Walter Müller, "Boundary condition effects in the simulation study of equilibrium properties of magnetic dipolar fluids," J. Chem. Phys. **119**, 379 (2003).